SUPPLEMENTARY INFORMATION

A High Resolution Association Mapping Panel for the Dissection of Complex Traits in Mice

Brian J. Bennett[1]*, Charles R. Farber[9]*, Luz Orozco[1]*, Hyun Min Kang[6]*, Anatole Ghazalpour[1], Nathan Siemers[7], Michael Neubauer[7], Isaac Neuhaus[7], Roumyana Yordanova[7], Bo Guan[7], Amy Truong[7], Wen-pin Yang[7], Aiqing He[7], Paul Kayne[7], Peter Gargalovic[8], Todd Kirchgessner[8], Calvin Pan[2], Lawrence W. Castellani[1], Emrah Kostem[5], Nicholas Furlotte[5], Thomas A. Drake[3], Eleazar Eskin[2,5≠], Aldons J. Lusis[1,2,4≠]

[1.] Department of Medicine/Division of Cardiology, [2.] Department of Human Genetics, and [3.] Department of Pathology and Laboratory Medicine, David Geffen School of Medicine at UCLA, University of California, Los Angeles CA

[4.] Department of Microbiology, Immunology and Molecular Genetics, and [5.] Department of Computer Science, UCLA, University of California, Los Angeles

[6]. Computer Science and Engineering, University of California, San Diego

[7.] Department of Applied Genomics, and [8.] Department of Atherosclerosis Drug Discovery, Bristol-Myers Squibb, Princeton, NJ

[9.] Department of Medicine, Department of Biochemistry and Molecular Genetics and Center for Public Health Genomics, University of Virginia, Charlottesville, VA 22908

[10]To whom correspondence should be addressed:
Aldons J. Lusis
Department of Medicine/Division of Cardiology
BH-307 Center for the Health Sciences
UCLA
Los Angeles, CA 90095-1679

Supplemental Figure Legends

Supplemental Figure 1: HMDP Yields High Resolution Expression Mapping. Several genes with previously reported expression QTL or SNPs causing differential variation in mouse strains are mapped. A. *St7* was previously shown to have an expression variation due to differential splicing(Schadt et al. 2003) B. *Hc* was previously reported to have a 2bp deletion leading to rapid decay of the transcript (Schadt et al. 2003). C. *Abcc6* expression is due to a SNP resulting in 5 bp deletion of *Abcc6* transcript resulting in altered splicing(Aherrahrou et al. 2008). D. *PiK3ap1* was validated using a cis/trans test(Doss et al. 2005). Red rectangles denote physical position of the gene.

Supplemental Figure 2: Estimated Resolution of HMDP for various SNP effect sizes. We simulated phenotypes for 10,000 SNPs in the HMDP at various effect sizes. Results represent the distance between the peak EMMA *p*-value assuming a 50% background genetic effect and the simulated SNP. A. SNP with 2.5% effect. B. SNP with 7.5% effect. C. SNP with 12.5% effect. D. SNP with 17.5% effect.

Supplemental Figure 3: Correcting for population structure dramatically reduces false positives in murine association studies Panel A is a histogram of uncorrected *p*-values for plasma HDL and panel B is a histogram EMMA corrected *p*-values for plasma HDL.

Supplemental Figure 4: Comparison of individual strain sets on HDL association mapping in the HMDP. High -resolution association mapping for HDL around the *Apoa2* locus on Chr 1 depicting individual RI panels (panels A-D), the inbred set (panel E) and the combined RI panels (panel F) and the complete HMDP (panel G) are shown.

Supplemental Figure 5: Variation in plasma lipid traits among the HMDP. A. Total Cholesterol, B. Triglycerides, and C. Unesterified Cholesterol.

Supplemental Figure 6: Genome Wide Association Mapping. Mapping of EMMA corrected *p*-values for A. Total Cholesterol, B. Triglycerides, and C. Unesterified Cholesterol.

Supplemental Figure 1

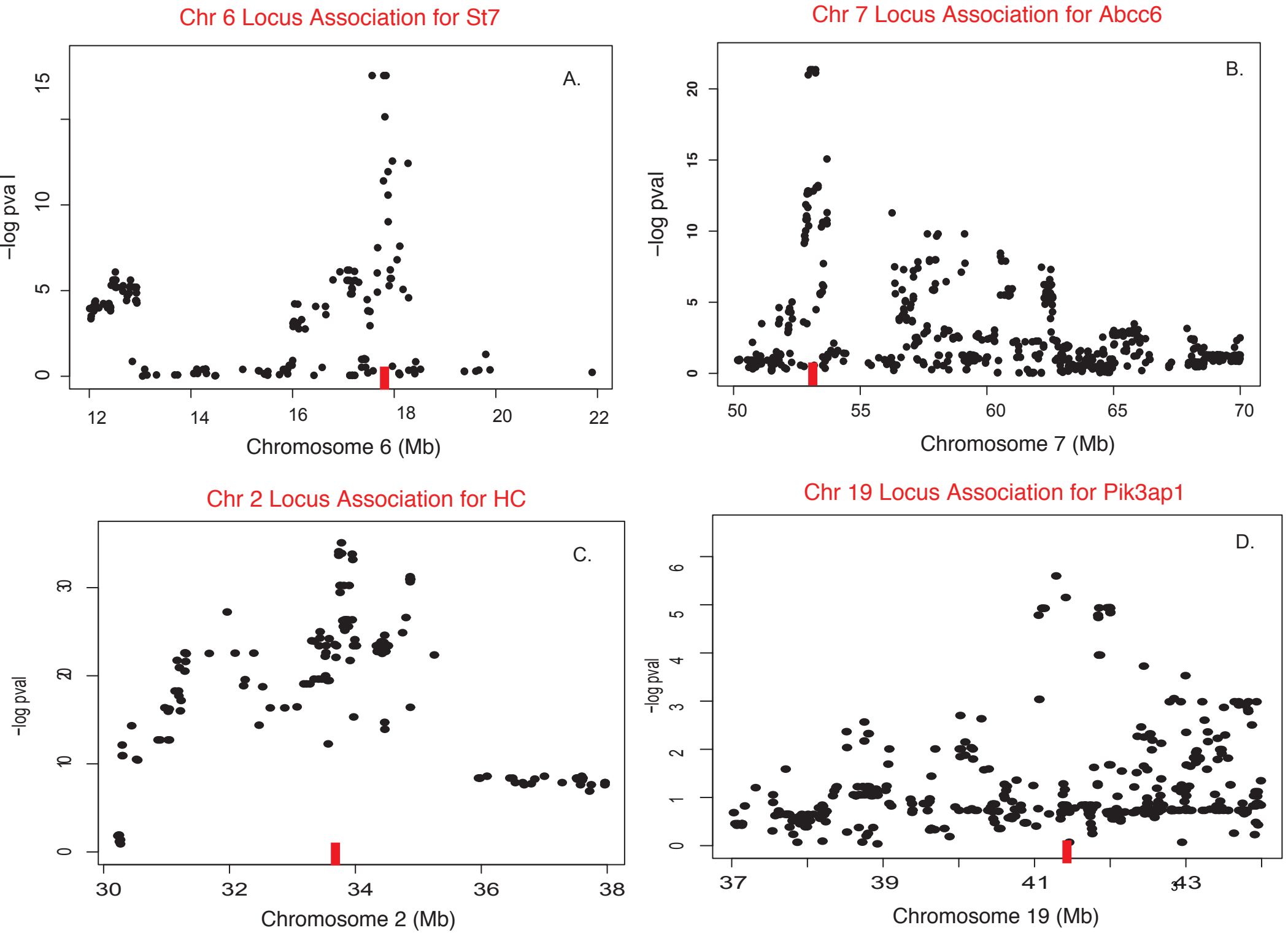

Supplemental Figure 2

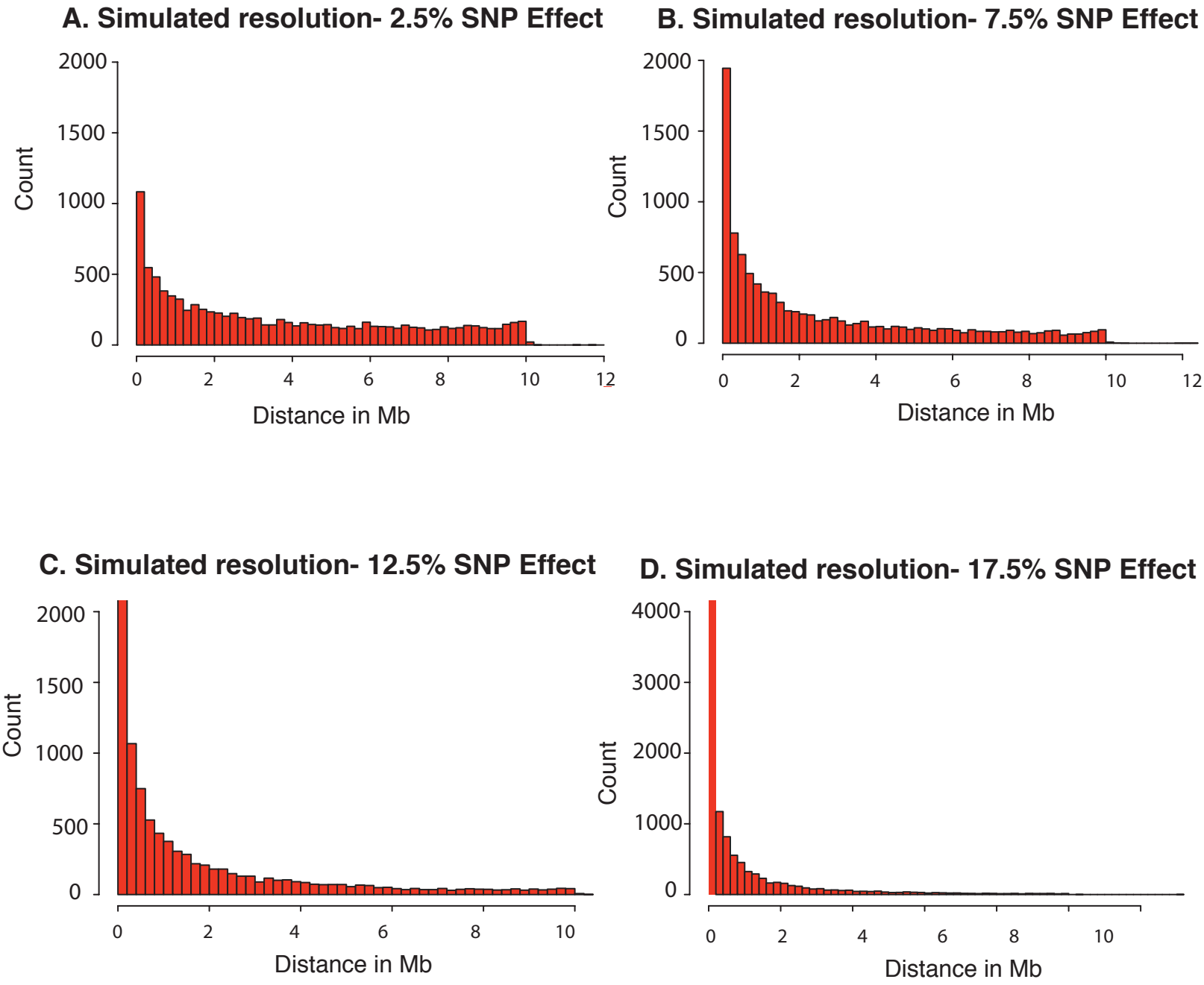

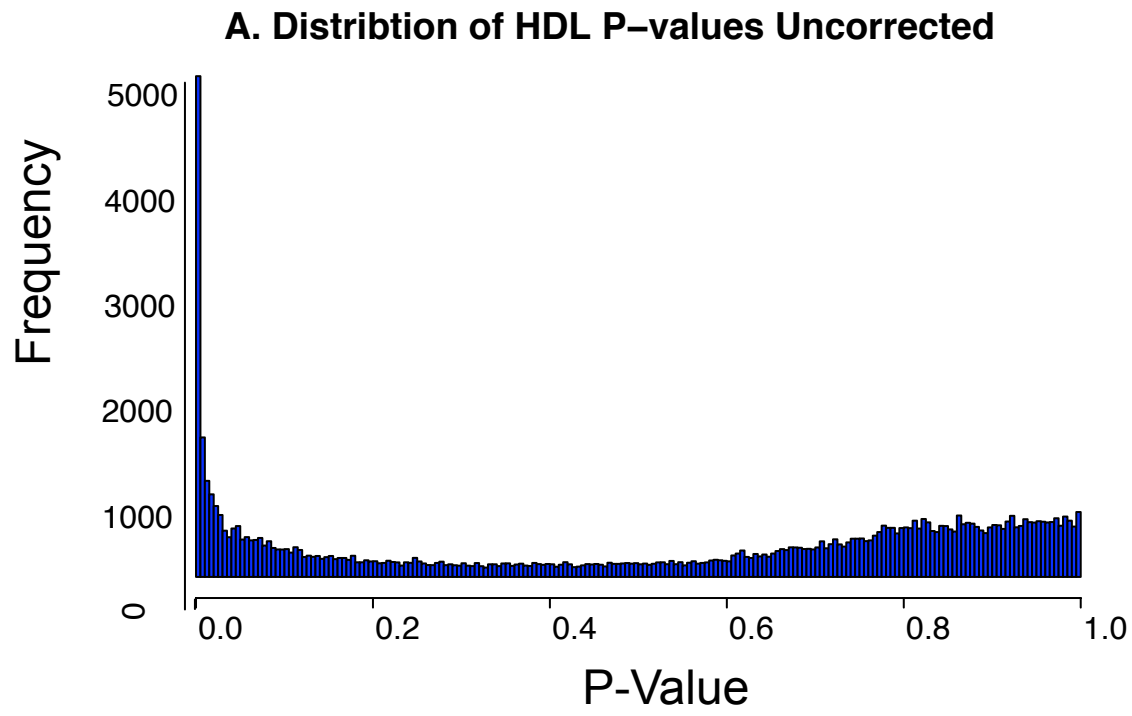
A. Distribtion of HDL P–values Uncorrected
Frequency
5000
4000
3000
2000
1000
0
0.0
0.2
0.4
0.6
0.8
1.0
P-Value

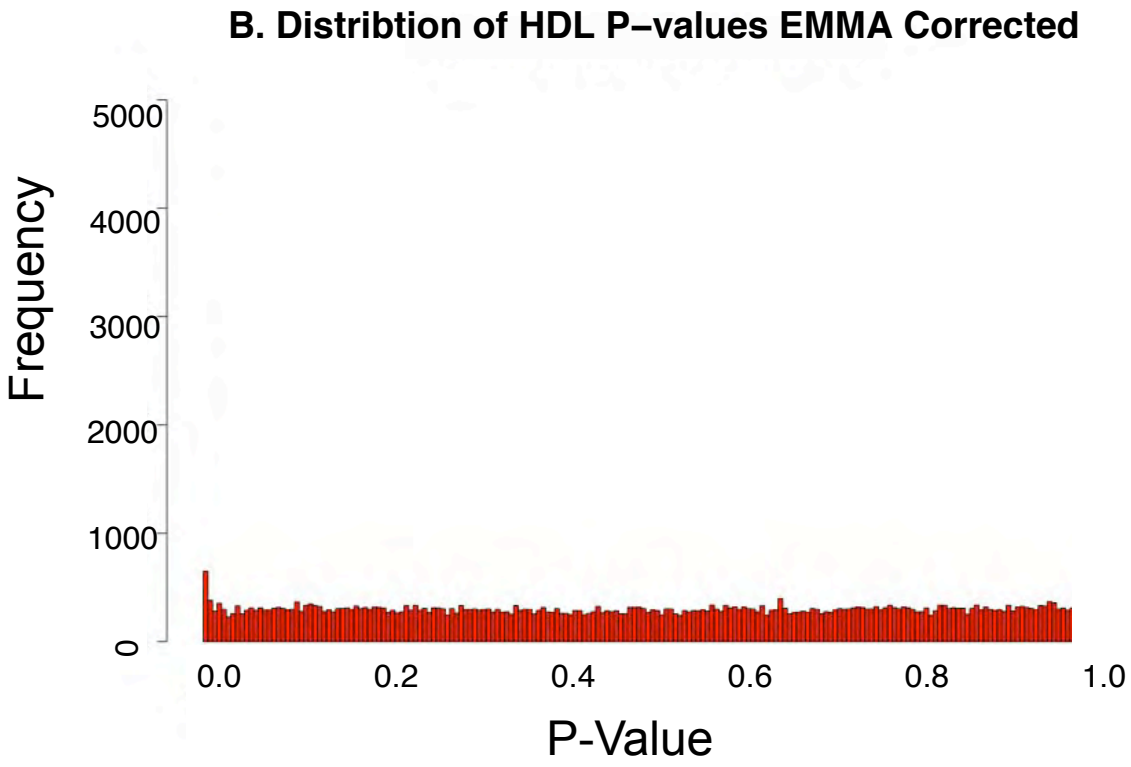
B. Distribtion of HDL P–values EMMA Corrected
Frequency
5000
4000
3000
2000
1000
0
0.0
0.2
0.4
0.6
0.8
1.0
P-Value

Supplemental Figure 4

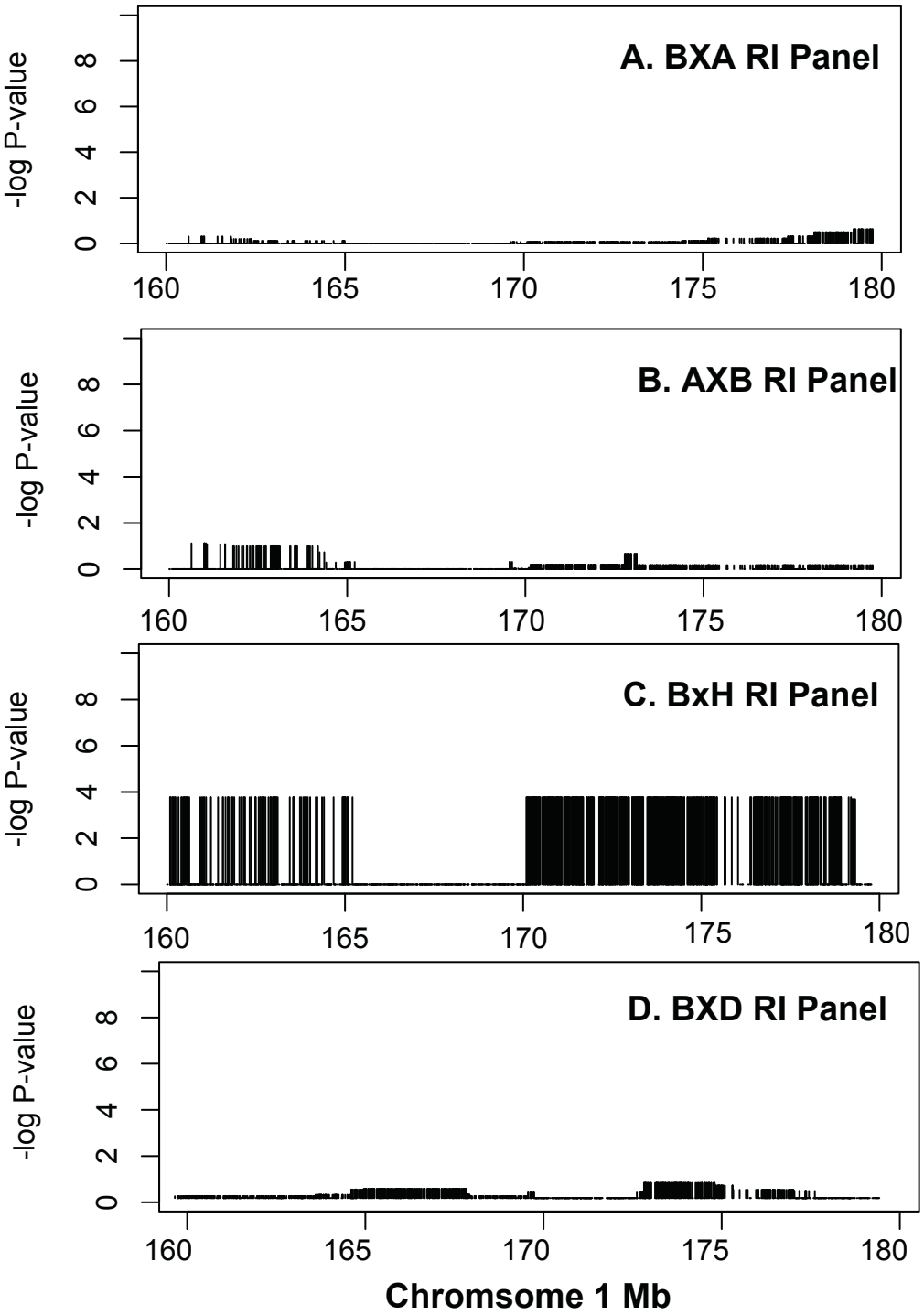

Supplemental Figure 5

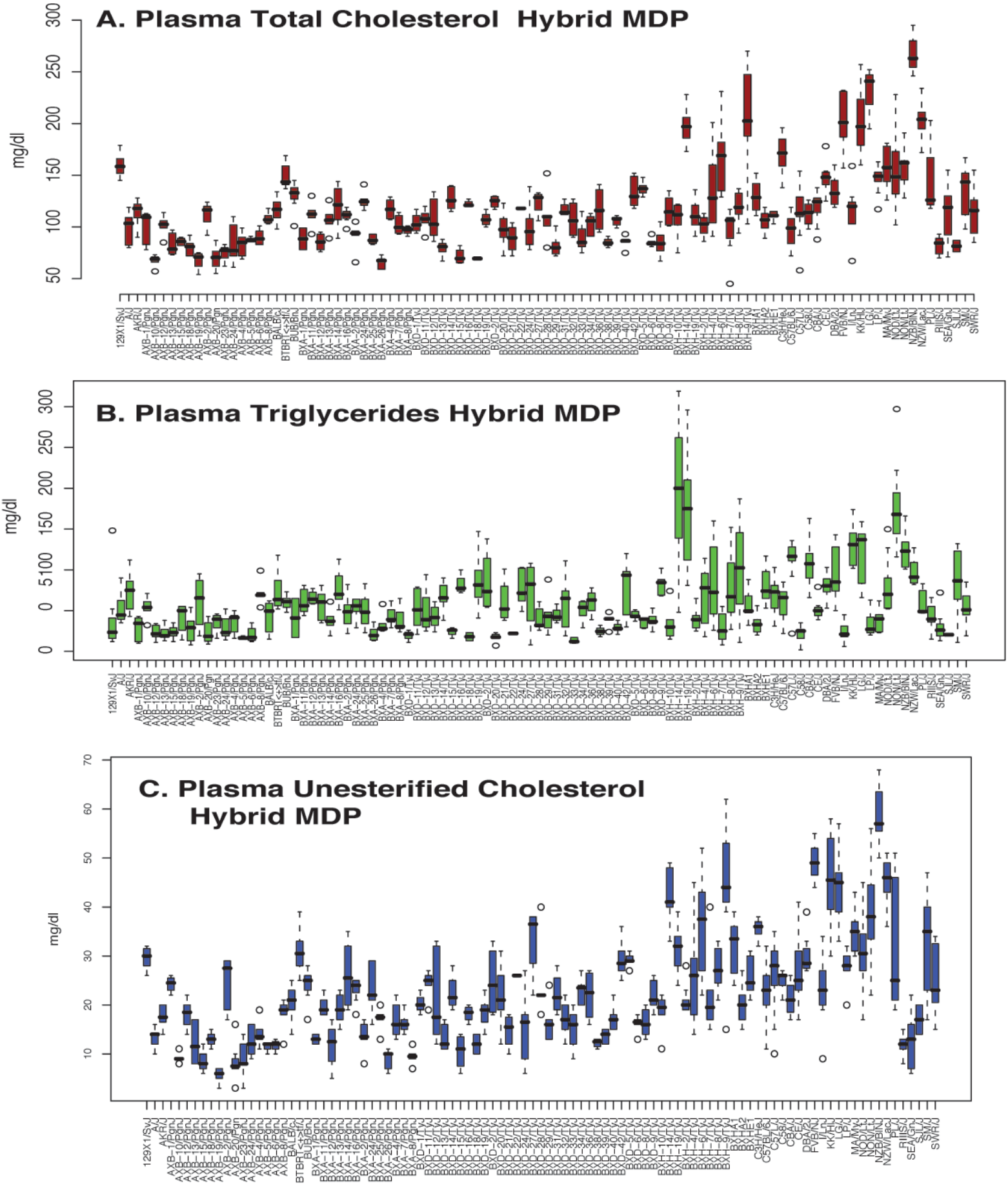

Supplemental Figure 6

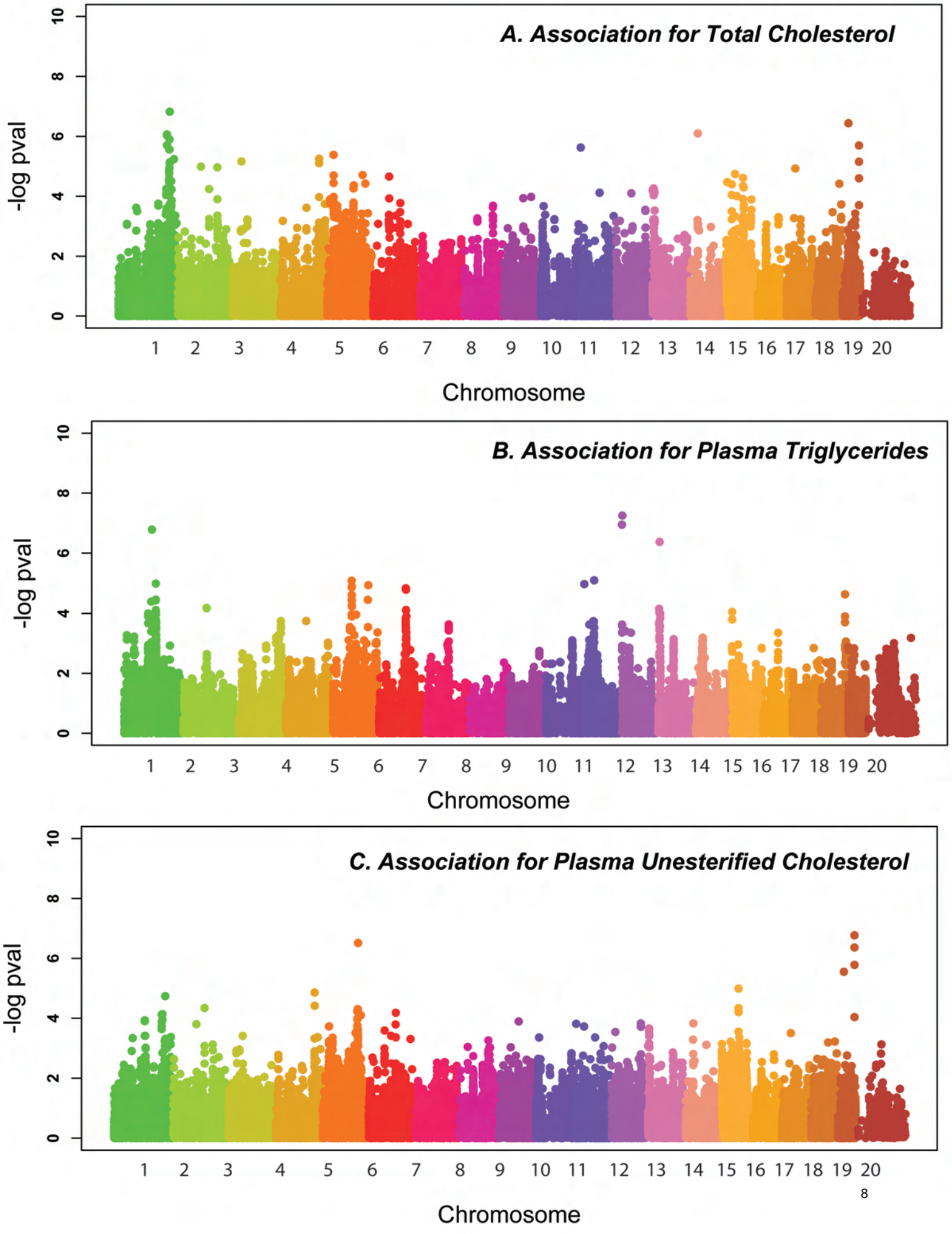

Supplemental Table 1. Inbred and RI strains used in mouse whole genome association. The numbers indicate total number of mice used for phenotyping

Inbred Strains		Recombinant inbred					
Strain	(n)	Strain	(n)	Strain	(n)	Strain	(n)
129X1/SvJ	10	AXB1/PgnJ	6	BXD1/TyJ	4	BXH14/TyJ	9
A/J	10	AXB10/PgnJ	5	BXD5/TyJ	6	BXH19/TyJ	18
AKR/J	10	AXB12/PgnJ	6	BXD6/TyJ	6	BXH2/TyJ	9
C57BL6/J	11	AXB13/PgnJ	4	BXD8/TyJ	6	BXH20/KccJ	8
BALB/cJ	10	AXB15/PgnJ	6	BXD9/TyJ	6	BXH22/KccJ	11
BTBR T+ tf/J	10	AXB19/PgnJ	6	BXD11/TyJ	6	BXH4/TyJ	11
BUB/BnJ	9	AXB19a/PgnJ	5	BXD12/TyJ	4	BXH6/TyJ	11
C3H/HeJ	10	AXB19b/PgnJ	8	BXD13/TyJ	4	BXH7/TyJ	10
C57L/J	11	AXB2/PgnJ	6	BXD14/TyJ	2	BXH8/TyJ	11
C58/J	10	AXB23/PgnJ	4	BXD15/TyJ	6	BXH9/TyJ	10
CBA/J	10	AXB24/PgnJ	5	BXD16/TyJ	4	B6Cc3-1/KccJ	6
CE/J	9	AXB4/PgnJ	6	BXD18/TyJ	6	BXH10/TyJ	6
DBA/2J	10	AXB5/PgnJ	2	BXD19/TyJ	5		
FVB/NJ	5	AXB6/PgnJ	6	BXD2/TyJ	2		
I/LnJ	9	AXB8/PgnJ	6	BXD20/TyJ	6		
KK/HiJ	8	BXA1/PgnJ	2	BXD21/TyJ	6		
LG/J	7	BXA11/PgnJ	6	BXD22/TyJ	5		
LP/J	10	BXA12/PgnJ	5	BXD24a/TyJ	5		
MA/MyJ	6	BXA13/PgnJ	6	BXD24b/TyJ	6		
NOD/ShiLtJ	10	BXA14/PgnJ	6	BXD27/TyJ	4		
NON/ShiLtJ	13	BXA16/PgnJ	7	BXD28/TyJ	8		
NZB/BINJ	7	BXA2/PgnJ	6	BXD29/TyJ	6		
NZW/LacJ	10	BXA24/PgnJ	6	BXD31/TyJ	6		
PL/J	10	BXA25/PgnJ	6	BXD32/TyJ	4		
RIIIS/J	10	BXA26/PgnJ	6	BXD33/TyJ	4		
SEA/GnJ	11	BXA4/PgnJ	6	BXD34/TyJ	6		
SJL/J	2	BXA7/PgnJ	6	BXD36/TyJ	6		
SM/J	10	BXA8/PgnJ	6	BXD38/TyJ	6		
SWR/J	10			BXD39/TyJ	6		
				BXD40/TyJ	6		
				BXD42/TyJ	6		

Supplemental Table 2 Statistical power of combined HMDP, each RI (BXD, BXA/AXB, BXH) set and classical inbreds (CI).

SNP effect : 10% variance, 5 replicates per strain (averaged), averaged power across 107k SNPs					
Strain sets	HMDP	BXD	BXA	BXH	CI
$h_g^2 = 0.00$	0.918	0.068	0.053	0.001	0.067
$h_g^2 = 0.25$	0.663	0.044	0.034	0.001	0.041
$h_g^2 = 0.50$	0.262	0.018	0.014	$<10^{-3}$	0.014
$h_g^2 = 0.75$	0.088	0.007	0.006	$<10^{-3}$	0.004
$h_g^2 = 1.00$	0.037	0.003	0.002	$<10^{-3}$	0.001
SNP effect : 20% variance, 5 replicates per strain (averaged), averaged power across 107k SNPs					
Strain sets	HMDP	BXD	BXA	BXH	CI
$h_g^2 = 0.00$	0.999	0.294	0.237	0.004	0.219
$h_g^2 = 0.25$	0.974	0.205	0.157	0.003	0.147
$h_g^2 = 0.50$	0.722	0.084	0.063	0.001	0.059
$h_g^2 = 0.75$	0.363	0.028	0.023	0.001	0.018
$h_g^2 = 1.00$	0.177	0.012	0.009	$<10^{-3}$	0.006

Supplemental Table 3. Top 100 *Cis*-eSNPs in identified in livers of MDP mice.

Affy Probe	Gene Symbol	*p*-Value	Chr	Position
1438644_x_at	Commd9	5.72E-155	2	102139130
1422000_at	Akr1c12	2.27E-113	13	3268047
1417208_at	Amacr	3.40E-113	15	11046878
1417461_at	Cap1	3.60E-100	4	122543559
1427651_x_at	LOC100045864	1.20E-98	17	35306154
1452544_x_at	LOC100045864	2.35E-98	17	35306154
1430979_a_at	Prdx2	7.23E-98	8	87596035
1425614_x_at	LOC100045864	1.47E-97	17	35306154
1456663_x_at	Tm2d2	3.42E-93	8	26014650
1425869_a_at	Psen2	2.17E-89	1	182107981
1418148_at	Abhd1	2.18E-88	5	31328124
1428004_at	3300001G02Rik	6.03E-88	11	32119734
1449635_at	Prpf19	7.30E-83	19	10991727
1423216_a_at	2510049I19Rik	4.98E-81	8	72635554
1437708_x_at	Vamp3	1.06E-80	4	150397589
1452464_a_at	Metapl1	9.61E-80	2	70987232
1425191_at	Ocel1	3.91E-78	8	73890792
1419327_at	Pdxdc1	2.46E-77	16	13922036
1430519_a_at	Cnot7	6.62E-77	8	41548800
1448622_at	Lsm4	3.00E-76	8	72270336
1434340_at	1110020P15Rik	4.05E-75	11	4613230
1419094_at	Cyp2c37	1.14E-74	19	40020044
1417462_at	Cap1	2.69E-74	4	122543559
1418837_at	Qprt	8.57E-74	7	134208755
1424576_s_at	Cyp2c44	3.29E-73	19	42872846
1425521_at	Paip1	7.39E-73	13	120070060
1433462_a_at	Pi4k2a	8.68E-73	19	41424882
1453571_at	Depdc6	5.48E-72	15	55001176
1437615_s_at	Vps37c	5.57E-72	19	10788815
1451602_at	Snx6	7.89E-72	12	55749395
1452705_at	Pdxdc1	6.47E-71	16	13856475
1425589_at	Hsd17b13	8.30E-71	5	104209865
1452302_at	Arhgef10	5.62E-70	8	15298046
1424039_at	Tmem66	2.60E-69	8	35199457
1422128_at	Rpl14	1.20E-68	9	119844975
1417619_at	Gadd45gip1	2.62E-66	8	87249570
1449526_a_at	Gdpd3	2.71E-66	7	133276153
1417264_at	Coq5	1.43E-65	5	115597885
1419637_s_at	4833420G17Rik	1.71E-65	13	120120533
1424454_at	Tmem87a	1.91E-65	2	121022064
1428267_at	Dhx40	2.35E-65	11	86564031
1430021_a_at	Sae1	3.12E-65	7	16868527

1436763_a_at	2310051E17Rik /// Klf9	4.91E-64	19	23460803
1423745_at	1110031B06Rik	9.50E-64	11	60806750
1424105_a_at	Pttg1	2.01E-63	11	42848308
1424138_at	Rhbdf1	5.53E-63	11	32119734
1422485_at	LOC100048076 /// Smad4	8.47E-63	18	74118720
1451667_at	C530043G21Rik	1.06E-62	1	158401038
1452303_at	Arhgef10	5.52E-62	8	15298046
1424893_at	Ndel1	6.37E-61	11	68659221
1421144_at	Rpgrip1	6.50E-61	14	54746094
1451346_at	Mtap	6.81E-61	4	88776714
1416709_a_at	Ngrn	1.89E-60	7	87216705
1449556_at	C920025E04Rik /// H2-T23 /// LOC100046736	2.52E-60	17	36637612
1454898_s_at	Iah1	7.03E-60	12	13234991
1415760_s_at	Atox1	1.91E-59	11	55307382
1425633_at	BC026782	2.91E-59	1	141917378
1419523_at	Cyp3a13	2.21E-58	5	138360832
1434348_at	Fez2	3.06E-58	17	78762552
1460639_a_at	Atox1	1.09E-57	11	55307382
1419636_at	4833420G17Rik	1.39E-57	13	120103562
1428013_at	6030458C11Rik	3.59E-57	15	12750495
1418989_at	Ctse	6.23E-57	1	133558515
1426921_at	Abcf1	8.31E-57	17	36100364
1423181_s_at	Clns1a	8.49E-57	7	105868232
1419017_at	Corin	1.04E-56	5	73225905
1426995_a_at	Gfer	1.14E-56	17	24497555
1438649_x_at	Pebp1	1.43E-56	5	117668111
1419407_at	Hc	3.41E-56	2	33778096
1429681_a_at	Gpsn2	7.45E-56	8	85955869
1436007_a_at	LOC100048066 /// Thumpd1	1.16E-55	7	127227636
1426450_at	Plcl2	2.03E-55	17	50464173
1419136_at	Akr1c18	2.05E-55	13	3268047
1416142_at	Rps6	2.38E-55	4	86568938
1422810_at	Zfp191	8.01E-55	18	24242822
1416443_a_at	Sae1	1.09E-54	7	16925841
1438220_at	Foxj3	3.65E-54	4	119189081
1433496_at	Glt25d1	8.12E-54	8	72331482
1433758_at	Nisch	3.15E-53	14	31943404
1428588_a_at	Mrpl41	3.71E-53	2	24993081
1437142_a_at	Pigo	1.00E-52	4	43274109
1430889_a_at	Tpmt	1.13E-52	13	47005930
1451731_at	Abca3	1.19E-52	17	24497555
1417265_s_at	Coq5	1.30E-52	5	115597885
1452231_x_at	Ifi203	1.57E-52	1	176081804

1424857_a_at	Trim34	2.60E-52	7	111733724
1433953_at	Zfp277	4.63E-52	12	41497934
1425336_x_at	H2-K1	4.87E-52	17	34607790
1425134_a_at	Pigx	8.33E-52	16	32016798
1426554_a_at	Pgam1	1.29E-51	19	41099412
1455918_at	Adrb3	2.86E-51	8	28679897
1419620_at	Pttg1	3.18E-51	11	42848308
1423867_at	Serpina3k	3.70E-51	12	105544118
1419436_at	Cfhr1	3.91E-51	1	142421123
1426753_at	Phf17	4.26E-51	3	42232091
1423554_at	Ggcx	1.59E-50	6	72230770
1424425_a_at	Mtap	1.63E-50	4	88776714
1416494_at	Ndufs5	2.48E-50	4	123026900
1434176_x_at	Poldip3	5.93E-50	15	83393007
1419635_at	4833420G17Rik	1.78E-49	13	120103562

Supplemental Table 4: HMDP Associations map to Loci Identified inQTL Studies

chr	bp	P_value	QTL name/Gene Name	peak linkage	Estimated Confidence Interval	LOD score	Distance between HMDP and QTL in Mb	MGI Link	
1	172.4	4.37E-10	Hdl34	171	NR (151 to 191)	11	1	MGI:3514357	(Machleder et al. 1997)
1	187	5.15E-07	Hdlq6	186	174 to 297	6	1	MGI:2448339	(Wang et al. 2003)
1	163.7	1.57E-06	Hdlq14	161	100 to 164	5.3	3	MGI:2448347	(Ishimori et al. 2004)
3	32	2.84E-06	Hdlq71	54	30 to 74	4.5	22	NA	(Su et al. 2009)
4	131	9.76E-06	Hdlq64	126	120 to 146	2.6 or 2.8	5	MGI:3720913	(Su et al. 2009) and (Stylianou et al. 2008)
5	23	7.93 E-06	Hdlq22	36	NR (16 to 56)	5.2	13	MGI:3041414	(Korstanje et al. 2004)
6	56	4.45E-06	Hdlq23	49	24 to 64	4.2	7	MGI:3041285	(Korstanje et al. 2004)
11	6.9	3.82E-09	none	NA			NA	NA	
14	33	1.28E-08	none	NA			NA	NA	
19	22	4.51E-06	Hdlq48	6.2	0 to 28		16	MGI:3618619	(Stylianou et al. 2006)

QTL Studies, QTL name, Peak Position and Confidence intervals were downloaded from MGI(http://www.informatics.jax.org/). Estimated confidence intervals where converted from cM to Mb by multiplying 2. NR means CI was not reported in original reference and was estimated to be peak marker± 20 Mb.

Supplemental Methods:

RNA isolation and Expression Profiling:

Initial profiling studies were performed on liver tissue. Flash frozen samples were weighed and homogenized in Qiazol according to the manufacturer's protocol. Following homogenization livers were isolated in RNeasy 96 columns (Qiagen) using the manufacturers protocol. RNA integrity was confirmed using the Agilent 2100 Bioanalyzer (Agilent, Palo Alto, CA).

Microarray Sample Preparation, Randomization: RNA was isolated from liver samples from the 99 strains comprising the HMDP. 92 strains of mice had three biological replicates, five strains had two biological replicates and two strains with one biological replicate each. All RNA samples were cleaned using a Biosprint96 (Qiagen, Valencia, CA) with RNA cleanup beads (Agencourt Bioscience, Beverly, MA) following manufacturer's protocol with adaptations for use with the Biosprint. The quality of the total RNA from the those samples were monitored by the Agilent 2100 Bioanalyzer (Agilent Technologies, Palo Alto, CA) and RNA quantity was measured with a NanoDrop (NanoDrop Technologies, Inc. Wilmington, DE) following the manufacturer's instructions. All samples were arrayed into three 96 well microtiter plates following a randomized design format that places samples from the same strain on different plates to better estimate variance across testing strains.

Microarray Target Labeling Hybridization, and Quality Control: All target labeling reagents were purchased from Affymetrix (Santa Clara, CA). Double-stranded cDNAs were synthesized from 1ug total RNA through reverse transcription with an oligo-dT primer containing the T7 RNA polymerase promoter and double strand conversion using the cDNA Synthesis System. Biotin-labeled cRNA was generated from the cDNA and used to probe Affymetrix Mouse Genome HT_MG-430A arrays. The HT_MG-430A Array plate consists of 96 single MG-430A arrays arranged into standard SBS 96 well plate format. All cDNA and cRNA target preparation steps were processed on a Caliper GeneChip Array Station from Affymetrix. Array hybridization, washing and scanning were performed according to the manufacturer's recommendations. Scanned images were subjected to visual inspection and a chip quality report was generated by the Affymetrix's GeneChip Operating System (GCOS) and Expression console (Affymetrix). Two of 288 chips were excluded due to low QC scores. The image data was processed using the Affymetrix GCOS algorithm utilizing quantile normalization or the Robust Multiarray method (RMA) to determine the specific hybridizing signal for each gene. Expression data can be obtained from Geo databases for liver (GSE16780)

Estimation of power and mapping resolution: The mapping resolution is evaluated using the *cis*-acting eQTLs. In addition to the eQTL mapping described above, we selected a subset of expression dataset involving BXD strains only, and performed association mapping. We evaluated the mapping resolution using the top 1,000 probes with strongest *cis*-acting eQTLs as the distance between the gene and

the strongest *cis*-eQTLs. When multiple SNPs are perfectly linked, the maximum distance is considered as the mapping resolution.

Genome Wide Expression Mapping: Each probeset was treated as an individual trait association analysis was performed and corrected for using EMMA. Since EMMA is orders of magnitude faster than other implementations commonly used, we were able to perform statistical analyses for all pairs of transcripts and genome wide markers in a few hours using a cluster of 50 processors. We further characterized the eQTL into distal or local eQTL. We defined an eQTL as local if the peak association signal was within a 10Mb sliding window of the gene(s) physical location. We then calculated the average distance between these *cis*-eEQTLs and transcription start site of the corresponding gene(s) transcription start site.

Comparison of HMDP to BXD subset: we selected a subset of expression dataset involving BXD strains only, and performed association mapping. We evaluated the mapping resolution using the top 1,000 probes with strongest *cis*-acting eQTLs as the distance between the gene and the strongest *cis*-eQTLs. When multiple SNPs are perfectly linked, the maximum distance is considered as the mapping resolution. For our simulations we picked 10,000 SNPs randomly from the set of SNPs polymorphic in each of the RI panels, BXD, BXA and BXH. This totaled approximately 35,000 SNPs. For each SNP, 5 replicates of 10 phenotypes were simulated with varying SNP effects while keeping the genetic background effect constant (50%). *P*-values were calculated using EMMA to account for population structure. A window 10Mb upstream and 10Mb downstream of each SNP was tested and the resolution was defined as the distance between the causal SNP and the SNP with the most significant p-value. When multiple SNPs are perfectly linked, the maximum distance is considered as the mapping resolution.

Genome-wide Significance Threshold: Genome-wide significance threshold in genome-wide association mapping is determined by the family-wise error rate (FWER) as the probability of observing one or more false positives across all SNPs per phenotype. Since the nearby SNPs are highly correlated with each other, applying Bonferroni correction imposing independence assumption among SNPs will lead to overly conservative estimate of significance threshold. Permutation test is a standard procedure to accurately account for multiple testing, but under the effect from population structure, permutation will break the relationship between the phenotype and the population structure and may lead an anti-conservative estimate of significance threshold. We used parametric bootstrapping to estimate the genome-wide threshold under various levels of population structure effect. It has been previously shown that parametric bootstrapping provide almost the same estimates of significance threshold (de Bakker et al. 2005). We confirmed it by comparing the genome-wide significance levels between permutation and parametric bootstrapping where the phenotypes are simulated by multivariate normal distribution. We ran 100 different sets of permutation test and parametric bootstrapping of size 1,000, and observed that the mean and standard error of the genome-wide significance threshold at FWER of 0.05 were $3.9e^{-6}\pm 0.3e^{-6}$, and $4.0e^{-6}\pm 0.3^{-6}$, respectively. This is approximately an order of magnitude larger than the

significance threshold obtained by Bonferroni correction ($4.6e^{-7}$). We also performed parametric bootstrapping under simulated the genetic background effect from population structure using EMMA. With 50% and 100% of variance explained by genetic background, the thresholds were determined to be $1.6e^{-6}\pm 0.2e^{-6}$ and $1.7e^{-6}\pm 0.2e^{-6}$. The reduction in the significance threshold compared to no genetic background effect is due to the fact that inter-SNP correlation due to long-range LDs reduces when conditioning on the population structure.

Because LD spans longer for RI strains than classical inbreds only or the HMDP panels, the significance threshold for a subset of the strains can dramatically differ. We used the parametric bootstrapping to estimate the significance threshold for each set of RI strains and classical inbreds. The estimated genome-wide significance threshold was $7.5e^{-5}\pm 0.5e^{-5}$ for BXD, $7.5e^{-5}\pm 0.4e^{-5}$ for AXB/BXA, and $1.1e^{-4}\pm 0.1e^{-4}$ for BXH, and $1.7e^{-6}\pm 0.2e^{-6}$ for classical inbreds. We used these thresholds to estimate the genome-wide power of each subset of strains in Figure 1 and Supplementary Table 3.

Supplemental References:

Aherrahrou, Z, Doehring LC, Ehlers EM, Liptau H, Depping R, Linsel-Nitschke P, Kaczmarek PM, Erdmann J, and Schunkert H. 2008. An alternative splice variant in Abcc6, the gene causing dystrophic calcification, leads to protein deficiency in C3H/He mice. *J Biol Chem* **283:** 7608-7615.

de Bakker, PI, Yelensky R, Pe'er I, Gabriel SB, Daly MJ, and Altshuler D. 2005. Efficiency and power in genetic association studies. *Nat Genet* **37:** 1217-1223.

Doss, S, Schadt EE, Drake TA, and Lusis AJ. 2005. Cis-acting expression quantitative trait loci in mice. *Genome Res* **15:** 681-691.

Ishimori, N, Li R, Kelmenson PM, Korstanje R, Walsh KA, Churchill GA, Forsman-Semb K, and Paigen B. 2004. Quantitative trait loci analysis for plasma HDL-cholesterol concentrations and atherosclerosis susceptibility between inbred mouse strains C57BL/6J and 129S1/SvImJ. *Arterioscler Thromb Vasc Biol* **24:** 161-166.

Korstanje, R, Li R, Howard T, Kelmenson P, Marshall J, Paigen B, and Churchill G. 2004. Influence of sex and diet on quantitative trait loci for HDL cholesterol levels in an SM/J by NZB/BlNJ intercross population. *J Lipid Res* **45:** 881-888.

Machleder, D, Ivandic B, Welch C, Castellani L, Reue K, and Lusis AJ. 1997. Complex genetic control of HDL levels in mice in response to an atherogenic diet. Coordinate regulation of HDL levels and bile acid metabolism. *J Clin Invest* **99:** 1406-1419.

Schadt, EE Monks SA Drake TA Lusis AJ Che N Colinayo V Ruff TG Milligan SB Lamb JR Cavet G et al. 2003. Genetics of gene expression surveyed in maize, mouse and man. *Nature* **422:** 297-302.

Stylianou, IM, Langley SR, Walsh K, Chen Y, Revenu C, and Paigen B. 2008. Differences in DBA/1J and DBA/2J reveal lipid QTL genes. *J Lipid Res* **49:** 2402-2413.

Stylianou, IM, Tsaih SW, DiPetrillo K, Ishimori N, Li R, Paigen B, and Churchill G. 2006. Complex genetic architecture revealed by analysis of high-density lipoprotein cholesterol in chromosome substitution strains and F2 crosses. *Genetics* **174:** 999-1007.

Su, Z, Ishimori N, Chen Y, Leiter EH, Churchill GA, Paigen B, and Stylianou IM. 2009. Four additional mouse crosses improve the lipid QTL landscape and identify Lipg as a QTL gene. *J Lipid Res*.

Wang, X Le Roy I Nicodeme E Li R Wagner R Petros C Churchill GA Harris S Darvasi A Kirilovsky J et al. 2003. Using advanced intercross lines for high-resolution mapping of HDL cholesterol quantitative trait loci. *Genome Res* **13:** 1654-1664.